



MODELING OF THERMAL STRESSES DESTROYING THE POROUS COATING OF HEAT-EXCHANGE SURFACES OF POWER PLANTS

A.A. Genbach¹, D.Yu. Bondartsev^{1,2}

¹Almaty University of Power Engineering and Telecommunications, Almaty, Republic of Kazakhstan

²JS Trest Sredazenergomontazh, Almaty, Republic of Kazakhstan
d.bondartsev@saem.kz

Abstract: Modeling of the low heat conductive low-porous capillary porous coatings and metal (copper, stainless steel) surfaces (base layer) was studied. Heat and mass transfer in the porous coatings moved with excessive liquid due to the combined action of capillary and mass forces. The dynamics of vapor bubble was described along with their heat-dynamic properties, which were observed by the optic research methods. Finding solution for the thermoelasticity allowed to reveal the influence of the specific heat flow and heat tension of compression and stretching depending on time of supply and sizes of pulled particles at the time of the system limit state as to "porous coating - base layer". The theory was confirmed by the trial, which was observed by camcorder SKS-1M.

Keywords: capillary-porous coatings, thermoelasticity, compression stresses, tensile stresses, model.

For citation: Genbach AA, Bondartsev DYu. Modeling of thermal stresses destroying the porous coating of heat-exchange surfaces of power plants. *Power engineering: research, equipment, technology*. 2019; 21(3):117-125. (In Russ). doi:10.30724/1998-9903-2019-21-3-117-125.

МОДЕЛИРОВАНИЕ ТЕРМИЧЕСКИХ НАПРЯЖЕНИЙ, РАЗРУШАЮЩИХ ПОРИСТЫЕ ПОКРЫТИЕ ТЕПЛООБМЕННЫХ ПОВЕРХНОСТЕЙ ЭНЕРГОУСТАНОВОК

А.А. Генбач¹, Д.Ю. Бондарцев^{1,2}

¹Алматинский Университет Энергетики и Связи, г. Алматы, Казахстан

²АО «Трест Средазэнергомонтаж», г. Алматы, Казахстан
d.bondartsev@saem.kz (<http://orcid.org/0000-0001-8778-7851>)

Резюме: Исследовано моделирование плохотеплопроводных малопористых капиллярно-пористых покрытий и металлических (медь, нержавеющая сталь) поверхностей (подложка). Тепломассоперенос в капиллярно - пористых покрытиях протекал с избытком жидкости за счет совместного действия капиллярных и массовых сил. Описана динамика паровых пузырей и их термогидравлические характеристики, наблюдаемые оптическими методами исследования. Разработана физическая модель процесса тепломассопереноса в реальной пористой структуре. Для такой модели решена задача термоупругости и определено предельное состояние системы хорошо - и плохотеплопроводных материалов

(пористое покрытие на металлической подложке). Определены тепловые потоки, подводимые к поверхности, время их воздействия на создание разрушающих напряжений, размеры отрывающихся частиц и глубины проникновения температурной волны в подложку. Тепловые потоки подсчитывались от времени взрывообразного появления первого зародыша (10^{-8} с) до времени разрушения материалов ($10^2 - 10^3$ с), т.е. от времени релаксации до времени, описывающего микропроцесс. С увеличением величины q в нагреваемом слое и, следовательно, уменьшением времени нагрева τ , растет роль напряжения сжатия. Несмотря на высокую сопротивляемость сжатию, разрушение от сжимающих термонапряжений происходит в более благоприятных условиях мгновенного и в малых объёмах. Теория подтверждена экспериментом, полученным в результате наблюдения камерой СКС-1М. Разрушение капиллярно-пористых покрытий происходит в результате потери устойчивости в тонком слое, прилежащем к свободной поверхности. Поэтому рассматривалось напряженное состояние верхнего слоя, толщина которого зависит от коэффициента теплоотдачи, структуры покрытия и подложки (металлической парогенерирующей поверхности).

Ключевые слова: капиллярно-пористые покрытия, естественные минеральные среды, термоупругость, напряжения сжатия, напряжения растяжения, модель, элементы энергоустановок, теплообмен.

The actual task in power plants is to create the degree of cooling of high-tension parts and assemblies. Modeling of capillary porous coatings and analogy of the processes taking place in them allow to reveal the mechanism of heat transfer at vaporization of liquids, to establish the zones of fatigue cracks occurrence and development in the centers of steam embryo activation, to study natural and artificial porous coatings applied to metal fences (substrates) up to the onset of the ultimate state of materials.

In our works [1-3] it is shown that different models given in [4-12] describe different modes of boiling and do not contradict each other.

On the basis of experimental and theoretical studies [4-12] dynamic models of heat transfer intensification at boiling on a porous surface are constructed. Developed surfaces contain tied internal cavities in the form of rectangular channels and small pores connecting the channels with the volume of liquid.

The ratio of the latent heat flow $\left(\frac{\pi}{6} \bar{D} r p \bar{n} \bar{f} \right)$ to the total heat flow could be larger (2 to 5) times for a developed surface than for a conventional surface with a specific heat flow up to 1×10^4 W/m². At high heat flows, this ratio decreased. The deviation of some data from estimated data reached 300%. The following indications are used in the formula: \bar{D} – average detachable diameter of vapor bubbles in the porous structure; r – specific heat of evaporation; p_v – vapor density; \bar{n} – average nucleation centers density; \bar{f} – average frequency of vapor bubble generation and silence.

Let's develop a physical model for transferring the specific heat flow q through the steam-generating surface (wall or substrate) which is covered by a capillary-porous structure (Fig. 1).

Processes of heat and mass transfer in the porous coating take place with the liquid overflow $\tilde{m} = m_l / m_v$ due to the action of the potential of pressure developed by capillary and mass forces ΔP_{cap+g} .

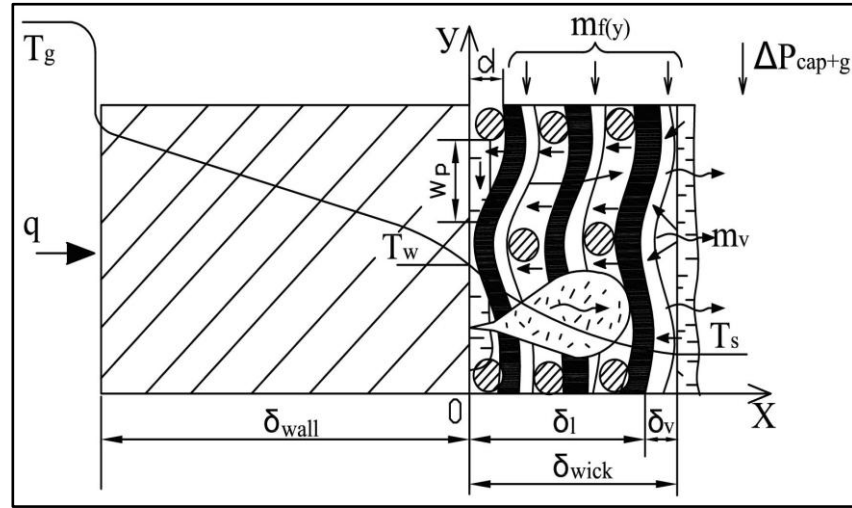


Fig. 3 Physical model of the heat and mass transfer in the real porous structure of coatings under the liquid overflow: Straight lines – fluid movement; wavy lines – steam movement: q – specific heat flow, W/m^2 ; T_g , T_w , T_s – temperatures of gases, wall (substrate) and saturation ($^{\circ}C$); δ_{wall} , δ_l , δ_v , δ_{wick} – thicknesses of wall, liquid, vapor, wick (m); $m_f(y)$, m_v – flows of liquid and steam, (kg/s); ΔP_{cap+g} – current dynamic capillary and mass pressure (N/m^2); d – grain size (m); w_p – width of the porous material cell (m).

In the cooling system under investigation, with small heat flows, heat is transferred due to conductive heat transmission; its value is the higher, the greater the effective thermal conductivity of the structure moistened with the liquid and the thermal conductivity of the shell. The fluid flow has a smooth nature; there are no vapor bubbles and related perturbation processes on the liquid surface. The liquid intensely evaporates from the menisci with small excesses of the coolant; when a liquid overflow increases, the evaporation begins from the surface of the flowing films.

In a certain heat flow that is smaller than the parameter $\tilde{m} = m_l / m_v$, a disruption in the smooth wavy flow of the liquid film begins, and separate vapor bubbles appear. Several active structure cells are constantly acting generation centers. The onset of liquid boiling ($\Delta T_{o.b.}$) depends on a lot of conditions and design parameters and is determined by the equation for this variation $\Delta T_{o.b.}$, which corresponds to the heat flow $q_{o.b.}$. The decrease in the flow rate of the cooling liquid $m_{l(y)}$ or the increase in the heat inflow q lead to a rapid growth of evaporation centers \tilde{n} .

A zone of transition to the developed bubble boil is not high due to the high rate of growth of the active vapor generation centers \tilde{n} . A further growth of the heat load q leads to the stable operation of a large number of active bubble generation centers and their uniform distribution throughout the steam-generating surface. However, certain critical conditions lead to a burnt-out and a surface burn-over. Therefore, the analogy in the processes of deliberate destruction of brittle materials and the burnt-out allows to model such processes and identify the mechanism thereof [1-3].

To learn the destruction process mechanism, experiments were carried out with the use of photoelasticity and holography methods [1]. The stress state of the models was estimated at similar times by photographic recording of isochromic patterns and counting the band order n at different points in the directions under study.

The solution of the problem of thermoelasticity makes it possible to determine the limit state of the medium for a porous coating and a metal vapor-generating surface [1-2].

In case of thermal destruction of poorly heat-conducting coatings with low porosity and a metal wall (substrate), it is required to identify the effect of the specific heat flux (q) applied to the surface and the time of its action τ on the formation of destructive stresses (σ), the granulometric

composition of shell (size of detached particles), as well as the depth of penetration of the temperature perturbation (δ) for the metal.

If q increases in a very short time interval (τ), the dynamic effects become very significant and compression stresses (σ_c) reach large values which are often several times higher than the tensile strength of the material in compression. Therefore, it is necessary to take into account these stresses in the mechanism of thermal destruction of the material. We have to find out what type of stress σ_i reaches before its limit values.

Let's consider a plate with the thickness of $2h$. The constant ultimate heat flux (q) is supplied to the surface $z = +h$, starting from the timepoint $t = 0$. The bottom surface $z = -h$ and the plate side edges are thermally insulated.

Thermal conductivity equation with limiting and initial conditions can be written in the form:

$$\alpha_w \frac{\partial T}{\partial z} = \frac{\partial T}{\partial \tau}, \quad T = 0, \quad \tau < 0 \quad (1)$$

$$\lambda_w \frac{\partial T}{\partial z} = q, \quad z = +h;$$

$$\lambda_w \frac{\partial T}{\partial z} = 0, \quad z = -h,$$

where α_w , λ_w – coefficients of thermal diffusivity and thermal conductivity of the wall (substrate).

The temperature distribution along the thickness depends on thermophysical properties of the material, its heat flux value and feeding time [2]:

$$T\left(\frac{z}{h}; \tau\right) = q \left\{ \frac{M}{2(c\lambda\rho)} \tau + \frac{\frac{3z}{h} + \frac{6z}{h} - 1}{12M} - \frac{4}{\pi M} \sum \frac{(-1)^n}{n} \exp\left[-n \frac{\pi M}{4(c\lambda\rho)} \tau\right] \cos\left[\frac{n\pi}{2}\left(\frac{z}{h} + 1\right)\right] \right\}, \quad (2)$$

where $M = \frac{\lambda_w}{h}$; n – positive numbers; c – heat capacity; ρ – wall density.

Using the known temperature distribution in the plate, we can find the thermal tension and compression stresses arising at a certain time t at various depths from the surface $\delta_i = (h = z_i)$ for a given value of the heat flux (q), since the plate with a variable temperature is in the plain stress condition.

$$\sigma_{xx} = \sigma_{yy} = -\frac{\alpha E}{(1-\nu)} T\left(\frac{z}{h}; \tau\right) + \frac{1}{(1-\nu)2h} \int \alpha E T\left(\frac{z}{h}; \tau\right) dz, \quad (3)$$

where the first term is the component of the compression stress, and the second term is the tension stress. α – linear expansion factor; E – Young's modulus (elasticity modulus); ν – Poisson ratio (lateral contraction);

If we are given the limit values of tension ($\sigma_{\text{lim.tens.}}$) and compression ($\sigma_{\text{lim.comp.}}$) stresses for coating and metal, we obtain the dependence of the heat flux (q) required for destruction, based on the time of supply (τ) and the depth of penetration (δ). In addition, when we equate temperatures on the plate surface to the melting temperature T_m of coating and metal, we find the values of specific heat fluxes necessary to melt the surface layer for a different period of action thereof (q_1), i.e. in each case, we have functional dependences of the heat flux on the time it affects the coating and the metal surface.

The causes of the destruction of boiler-turbine parts depend on the prehistory of the development of cracks in the stress raiser (relaxation zone) [4-8, 9-12]. Counting must be conducted from the time of the explosive appearance of the nucleating center of vapor (the time interval is 10^{-8} s to 10^{-3} s). The energy of the spontaneous appearance of a vapor bubble is a value close to the value which is constant (invariant) with respect to time of its growth. It is spent to maintain the nucleating center with a radius of R_{kr} and prevents it from collapsing (q reaches up to 10^8 W/m²). At this time interval, a thermodynamic equilibrium is established for the transition from microprocesses (microparticles and clusters with sizes of $(10^{-7} \div 10^{-8})$ m (nanoparticles) of separate (single) individual bubbles to processes described by the behavior of a large number of bubbles, using integrated characteristics ($\bar{q}, \bar{\alpha}, \bar{\Delta T}, \bar{\Delta P}, \bar{w}$), where $\bar{\alpha}, \bar{\Delta T}, \bar{\Delta P}, \bar{w}$ is average values of heat transfer coefficients, temperature and hydro-gas dynamic pressures and flow velocity. The presence of stress concentrators where the active vapor phase is generated, significantly reduces the $\sigma_{lim.comp.}/\sigma_{lim.tens.}$ ratio, and this value can be equal $(1 \div 2)$, including for energy steels. We have also to take into account the presence of other stress raiser, the cyclicity of loads during starting and stopping modes of equipment operation, which lead to fatigue cracks (stresses). Consequently, there's a high possibility that $\sigma_{lim.tens.} \approx \sigma_{lim.comp.}$, and $\sigma_{lim.tens.}$ reaches 10 MPa and becomes of the same order for porous coatings.

The processes of death as well as the nucleation have also explosive nature ($\tau = 10^{-8} \div 10^{-6}$ s), which leads to the emergence of cumulative phenomena, which along with the corrosive and electrical processes destroy the stress raiser (active generation center) due to erosion processes, bringing its size to the critical crack. In the case of instant condensation of vapor in the cavity (hole), its volume instantaneously disappears and a powerful cumulative effect (cavitation) is formed. In this case, shock waves penetrate into the parts and cracks develop, where an oxygen enters.

At the moment of "birth" of a bubble or a drop, α is up to 1×10^5 W/m² at a vapor temperature $(500 \div 565)$ °C, ΔT reaches 500 °C, and q values acting at the bottom of the bubble ("dry" spot zone) is up to 5×10^7 W/m². If we take into account that the individual vapor bubble generates q 10 times more than its integral value [3], then the total q is 5×10^8 W/m², which is represented in $q = q(\tau, \delta)$ in the figures. The greater the penetration depth of the heat wave (or δ of the detached particle from the porous coating), the longer it will take to destroy the parts by stresses (Figures 2-4).

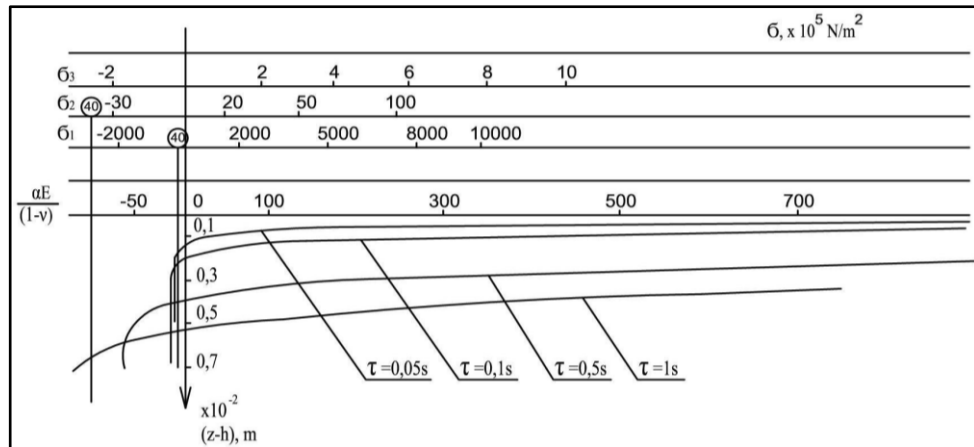


Fig. 2 Stress diagrams σ_i for the quartz plate (coating) thickness for various heat fluxes q_i and the time of their action τ : $q_1 = 8.8 \times 10^7$ W/m²; $q_2 = 0.12 \times 10^7$ W/m²; $q_3 = 0.008 \times 10^7$ W/m²; 40 – yield strength

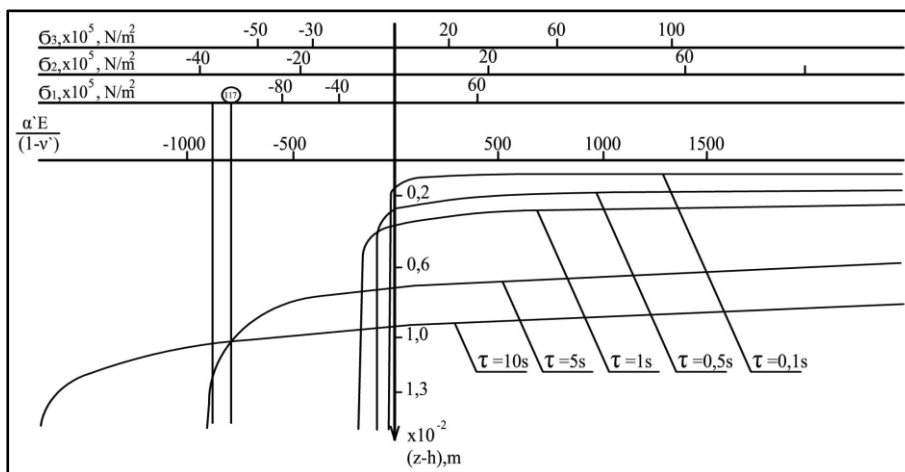


Fig. 3 Stress diagrams for granite coating thickness for different heat fluxes q_i and time τ of their action:
 $q_1 = 0.142 \times 10^7 \text{ W/m}^2$; $q_2 = 0.042 \times 10^7 \text{ W/m}^2$; $q_3 = 0.0075 \times 10^7 \text{ W/m}^2$;
 117 – yield strength: $\sigma_i = \times 10^5 \text{ H/m}^2$, $E = \times 10^5 \text{ H/m}^2$.

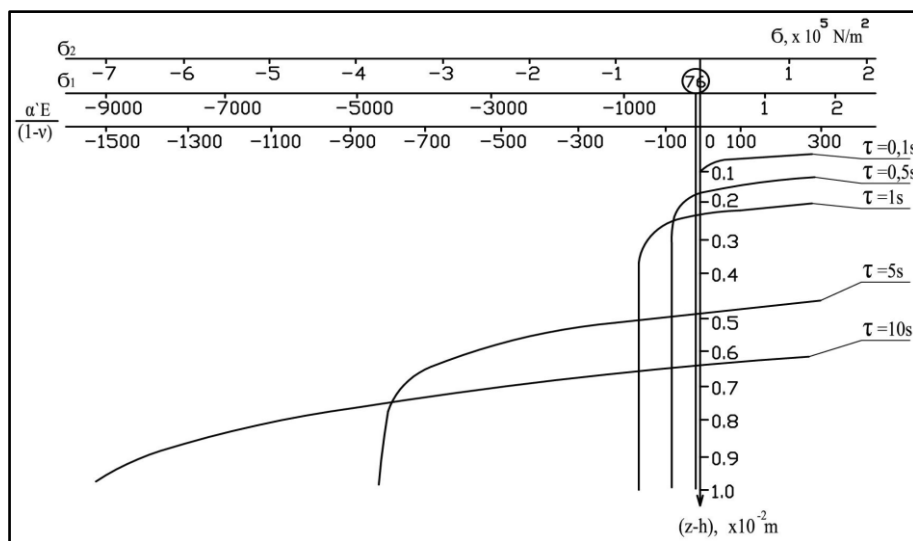


Fig. 4 Stress diagrams for the teschenite plate (coating) thickness for different q_i and τ values:
 $q_1 = 6.6 \times 10^6 \text{ W/m}^2$; $q_2 = 0.1 \times 10^4 \text{ W/m}^2$; 76 – yield strength

The relationship between compressive and tensile stresses is shown in Fig. 2-4. It is stress diagrams (coating) within the plate for various time intervals from the beginning of the process under consideration. At small values of τ and order of 10^{-2} s, only compression stresses arise. Starting from $\tau \sim 10^{-1}$ s, in some region of $\Delta (h-z_i)$, the compression stress turns into a tensile stress, and for different time intervals it is at different depths from the plate surface.

With an increase in q in the heated layer, and consequently a decrease in the heating time τ , the role of the compression stress increases. Despite the high resistance to compression, the destruction from compressive thermal stresses occurs under more favorable conditions of instantaneously and in small volumes.

For heated vapor-generating surfaces, the film boiling was established and the temperature of the surface increased sharply to a value T_m , as a result of the change in the boiling condition.

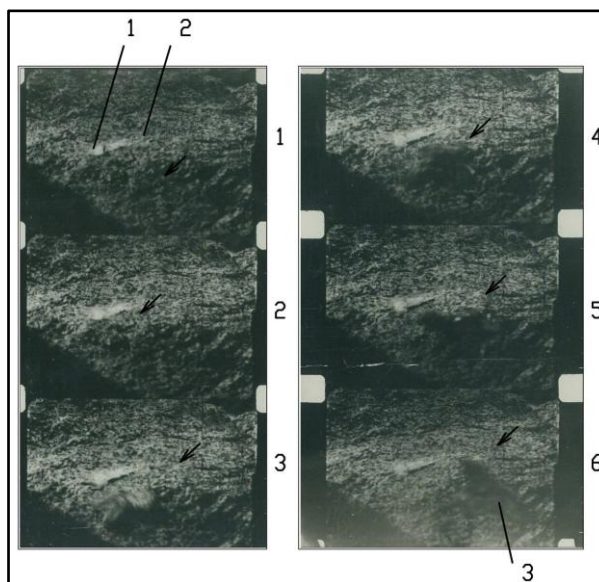


Fig. 5. Fragment of a high-speed shooting of the destruction of a teshenite with a rocket flame-jet burner with a specific heat flux equal to $1.2 \times 10^6 \text{ W/m}^2$. A shell with a size of 2.5×10^{-3} forms for 2.2 s.

A line of destruction of "equal possibilities" is clearly visible (arrow): 1 – capillary-porous coating; 2 – particle (shell) detached from the coating; 3 – line of destruction of "equal possibilities". Cinemagram of particle flight in time: τ_1 to τ_6 : 1 = 0 s; 2 = 5/1500 s; 3 = 10/1500 s; 4 = 15/1500 s; 5 = 20/1500 s; 6 = 25/1500 s.

A calculation was made of the specific energy (Q) of the destruction of a unit volume of quartz, granite, and teshenite coatings. The energy Q was calculated, depending on the thickness δ of the detached particles. Curves have pronounced minima.

For quartz coating, the minimum energy loss is $Q=0.5 \times 10^9 \text{ J/m}^3$ for $\tau = (0.1 \div 1) \text{ s}$, $\delta_i = (0.1 \div 0.25) \times 10^{-2} \text{ m}$.

For granite coating: $Q=2.5 \times 10^9 \text{ J/m}^3$ for $\tau = (0.1 \div 5) \text{ s}$, $\delta_i = (0.1 \div 0.3) \times 10^{-2} \text{ m}$. For $q=0.1 \times 10^7 \text{ W/m}^2$ and $\delta = (0.2 \div 1.5) \times 10^{-2} \text{ m}$, $Q = 2.5 \times 10^9 \text{ J/m}^3$.

For teshenite coating: $Q=0.5 \times 10^9 \text{ J/m}^3$ for $\tau = (0.1 \div 5) \text{ s}$, $\delta_i = (0.1 \div 0.4) \times 10^{-2} \text{ m}$, where the ratio of limit normal compression and tensile stresses varied from 20 to 30. The presence of microcracks in the coating monolith reduces its compressive strength in the vicinity of this crack so that the compressive strength can be only 2 times greater than the tensile strength.

Curves ($Q = f(q)$) with their minima with increasing of δ_i move in the direction of the decrease in q , and for the thermal destruction of brittle coatings, a lower energy capacity Q is required.

Conclusion

The danger of the appearance of limit thermal stresses is great at the moment of startup and shutdown of power equipment at power plants. These stresses arise primarily in the places of concentrators, which are active vapor phase centers or condensate formation centers. The capillary-porous structure can be both of natural origin (salt deposits, tarnishes) and artificially created with well and poorly heat-conducting materials in a wide range of porosity and permeability of 3% to 90%. Structures can play a modeling role and serve as a high-intensity and forced cooling system. For example, teshenite porous coatings with a 5-fold greater lineal expansion coefficient and a 10-fold lower thermal conductivity factor and approximately the same melting point in comparison with energy steels serve as a modeling material. They are the most viscous with a porosity of up to 30%.

References

1. Genbach A.A., Bondartsev D.Yu., Iliev I.K. Heat transfer crisis in the capillary-porous cooling system of elements of heat and power installations. *Thermal Science* 2019; 23(Pt2):849-860. <https://doi.org/10.2298/TSCI171016139G>
2. Genbach A.A., Bondartsev D.Yu., Iliya K. Iliev. Investigation of a high-forced cooling system for the elements of heat power installations. *Journal of machine Engineering* . 2018; 18 (2):106-117.
3. Genbach A.A., Bondartsev D.Yu., Iliev I.K. Modelling of capillary coatings and heat exchange surfaces of elements of thermal power plants. *Bulgarian Chemical Communications*. 2018; 50:133-139. doi:10.5604/01.3001.0012.0937.
4. Jamialahmadi M. Experimental and Theoretical Studies on Subcooled Flow Boiling of Pure Liquids and Multicomponent Mixtures, *Intern. J Heat Mass Transfer*. 2008; 51 (9-10): 2482–2493 doi: 10.1016 / j.ijheatmasstransfer.2007.07.052.
5. Ose Y., Kunugi T. Numerical Study on Subcooled Pool Boiling, *Progr. In Nucl. Sci. and Technology*, 2011; 2:125–129.
6. Krepper E. CFD Modeling Subcooled Boiling-Concept, Validation and Application to Fuel Assembly Design, *Nucl. Eng. and Design*, 2007; 237 (7.):716–731. doi: 10.1016 / j.nucengdes.2006.10.023
7. Ovsyanik A.V. Modelirovanie processov teploobmena v kipyashchih zhidkostyah, Gomel'skij gosudarstvennyj tekhnicheskij universitet im. P.O. Suhogo, Gomel': Belarus', 2012. (In Russ).
8. Alekseik O.S., Kravets V.Yu. Physical Model of Boiling on Porous Structure in the Limited Space. *Eastern-European Journal of Enterprise Technologies*. 2013; 64 (4):26–31.
9. Polyayev V.M., Majorov V.A., Vasil'ev L.L. *Gidrodinamika i teploobmen v poristyh elementah konstrukcij letatel'nyh apparatah*. M.: Mashinostroenie 1998. (In Russ).
10. Kovalev S.A., Solov'ev S.L. *Isparenie i kondensaciya v teplovyh trubah*. M.: Nauka, 1989. (In Russ).
11. Kupetz M., Heiew Jeni E., Hiss F. Modernization and prolongation of operation of steam turbine power plants in Eastern Europe and Russia / *Thermal Engineering*. 2014; 6: 35–43. (In Russ.)
12. Grin' E.A. Vozmozhnosti mekhaniki razrusheniya primenitel'no k zadacham prochnosti, resursa i obosnovaniya bezopasnoj ekspluatatsii teplomekhanicheskogo energooborudovaniya. *Teploenergetika*. 2013; 1:25–32. (In Russ).

Литература

1. Genbach A.A., Bondartsev D.Yu., Iliev I.K. Heat transfer crisis in the capillary-porous cooling system of elements of heat and power installations. // *Thermal Science*. 2019. Vol. 23, Pt 2 A, pp. 849-860.
2. Genbach A.A., Bondartsev D.Yu., Iliev I.K. Investigation of a high-forced cooling system for the elements of heat power installations, *Journal of machine Engineering*, 2018. Vol. 18, №2. pp. 106-117.
3. Genbach A.A., Bondartsev D.U., Iliev I.K. Modelling of capillary coatings and heat exchange surfaces of elements of thermal power plants. // *Bulgarian Chemical Communications*, 2018. Vol. 50, Special Issue G. pp. 133 – 139.
4. Jamialahmadi M.. Experimental and Theoretical Studies on Subcooled Flow Boiling of Pure Liquids and Multicomponent Mixtures, *Intern. // Heat Mass Transfer*. 2008. Vol. 51, № 9-10. pp. 2482-2493.
5. Ose Y., Kunugi T. Numerical Study on Subcooled Pool Boiling, *Progr. In Nucl. Sci. and Technology* 2011. Vol 2, pp. 125-129.
6. Krepper E. CFD Modeling Subcooled Boiling-Concept, Validation and Application to Fuel Assembly Design, *Nucl. Eng. and Design* 2007, Vol 237. N7. pp. 716-731.
7. Овсяник А.В. Моделирование процессов теплообмена в кипящих жидкостях, Гомельский государственный технический университет им. П.О. Сухого, Гомель: Беларусь, 2012. 260 с.
8. Alekseik, O.S., Kravets V. Yu. Physical Model of Boiling on Porous Structure in the Limited Space. // *Eastern-European Journal of Enterprise Technologies*, 2013 64(4), pp. 26-31.
9. Поляев В.М., Майоров В.А., Васильев Л.Л. Гидродинамика и теплообмен в пористых элементах конструкций летательных аппаратах. М.: Машиностроение, 1998. – 168 с.
10. Ковалев С.А., Соловьев С.Л. Испарение и конденсация в тепловых трубах. – М.: Наука, 1989. 112 с.
11. Kupetz M., Jeni Heiew E., Hiss F. Модернизация и продление срока эксплуатации паротурбинных электростанций в Восточной Европе и в России. // *Теплоэнергетика*. 2014. № 6. С. 35-43.
12. Гринь Е.А. Возможности механики разрушения применительно к задачам прочности, ресурса и обоснования безопасной эксплуатации тепломеханического энергооборудования // *Теплоэнергетика*. 2013. №1. С. 25-32.

Authors of the publication

Alexsandr A. Genbach - doctor of technical sciences, professor, department of thermal power plants, "Almaty University of Power Engineering and Telecommunications" (AUPET).

David Yu. Bondartsev - doctoral PhD, department of thermal power plants, "Almaty University of Power Engineering and Telecommunications" (AUPET), lead engineer of JS "Trest Sredazenergomontazh" (production planning and control department).

Received

November 02, 2018